Monte Carlo Analyses of X-Ray Absorption, Noise, and Detective Quantum Efficiency Considering Therapeutic X-Ray Spectrum in Portal Imaging Detector

Gyuseong Cho, *Member, IEEE*, Ho Kyung Kim, Yong Hyun Chung, Do Kyung Kim, Hyoung Koo Lee, Tae Suk Suh, and Koan Sik Joo

***Abstract*—The Bremsstrahlung spectrum from a 6-MV linear accelerator (LINAC) was obtained and used as an input X-ray source in the simulation to estimate several important physical quantities of the detector in a therapeutic X-ray portal imaging system, such as quantum and energy absorption efficiencies, Swank factor, and detective quantum efficiency (DQE). In addition, we have obtained a spatial distribution of energy deposit within the detector, resulting in a spatial-frequency-dependent DQE. From the simulation results, it is found that the use of metal plate largely enhances the energy absorption, leading to a large output signal. However, considering the noise properties, the presence of a metal plate degrades the DQE at nonzero spatial frequencies because the detector absorption noise is dominated by the quantum absorption. We have verified our simulation results by comparison with experimental measurements and results from other works.**

I. Introduction

MANY different types of electronic portal imaging devices (EPIDs) have been developed as alternatives to the conventional X-ray film used for the verification of radiation field placement in external radiation therapy, such as the matrix ion chamber, video-based EPID, and, most recently, flat-panel type devices (amorphous silicon- or selenium-based pixel detectors) [1]. Among them, the video-based EPID is the most widely used now due to its simple and inexpensive fabrication with the use of charge-coupled devices (CCDs) or a complementary metal–oxide–semiconductor (CMOS) image sensor, which gives higher resolution and sensitivity at low cost.

In a video-based EPID, a phosphor screen pasted to a metal plate, as an X-ray converter or so-called portal detector, as the first stage in the cascaded imaging chains transferring anatomical information to the final user. Therefore, it is largely responsible for the total performance of the system. Several theoretical and experimental studies for the optimal design of the metal plate/phosphor screen combination have been performed [2]–[7]. However, those studies were based on simple approximations—for example, a monoenergetic X-ray beam as the input. Also, some papers consider detective quantum efficiency (DQE) only at zero frequency [2], [4].

Based on Monte Carlo technique, we have investigated the overall performance of the portal detector in terms of X-ray absorption and associated noise characteristics considering the Bremsstrahlung spectrum from a 6-MV linear accelerator (LINAC). In addition, we simulated the spatial distribution of the energy deposit within the detector, resulting in a frequency-dependent DQE or DQE(f). The simulation results will be discussed in comparison with experimental measurements and other results in the literature.

II. Material and Methods

The phosphor film is the first signal transfer stage in an X-ray imaging system. Its performance is characterized by many terms, such as energy absorption efficiency, detective quantum efficiency, noise power spectrum, modulation transfer function, etc. Swank [8] and Jaffray *et al.* [4] have described these properties using energy moments of the absorbed energy distribution (AED) in the case of monoenergetic X-ray beams.

The AED is the distribution of deposited energy from each X-ray quantum in the phosphor film through interaction mechanisms such as photoelectric absorption, Compton scattering, and pair production. The AED is difficult to measure directly, so it is normally simulated by Monte Carlo techniques. The deposited or absorbed energy cannot exceed the energy of the incident X-ray. Once we know the AED, we can calculate its energy moments of various degrees by the following equation:

$$M_n = \int_E S(E)E^n dE \tag{1}$$

where

E amount of X-ray energy absorbed by the film;
$S(E)$ the AED;
M_n nth moment.

Based on this expression, we can describe several physical quantities important in estimating the performance of the phosphor

Manuscript received October 13, 2000; revised May 4, 2001.

G. Cho, H. K. Kim, and Y. H. Chung are with the Department of Nuclear Engineering, Korea Advanced Institute of Science and Technology, Taejon 305-701, South Korea.

D. K. Kim is with the Department of Material Engineering, Korea Advanced Institute of Science and Technology, Taejon 305-701, South Korea.

H. K. Lee and T. S. Suh are with the Department of Biomedical Engineering, Catholic University Medical College, Seoul 137-040, South Korea.

K. S. Joo is with the Department of Physics, Myonji University, Yonin 449-728, South Korea.

Publisher Item Identifier S 0018-9499(01)08658-0.

film as an X-ray detector as follows:

$$A_Q = M_0 \tag{2}$$

$$A_E = \frac{M_1}{M_0} \tag{3}$$

$$A_S = \frac{M_1^2}{M_0 M_2} \tag{4}$$

$$\mathrm{DQE} = \frac{M_1^2}{M_2} \tag{5}$$

where A_Q, A_E, and A_S represent quantum absorption, energy absorption, and Swank or statistical factor, respectively.

We took this approach but extended it to polyenergetic X-ray beams. The AED of a phosphor film from X-rays having the energy spectrum of $\Phi(E)$ is simply expressed by the following integral [9]:

$$S(E) = \int_0^{E_0} \Phi(E') R(E, E') dE' \tag{6}$$

where E_0 is the maximum energy in the spectrum and the kernel $R(E, E')$ is the response function of the phosphor, which is the probability that a single incident X-ray quantum with energy E' will deposit the amount of energy E within the detector.

As the first stage of analysis, a Bremsstrahlung spectrum from the gold target of a 6-MV LINAC[1] (incident electron kinetic energy of 5.58 MeV), $\Phi(E')$, was simulated by MCNP4B code [10] based on the material and geometric data [11] as an incident X-ray source in the simulation.

Then, to calculate the AED of the phosphor, we considered a pencil beam incident perpendicularly onto the portal detector with the Bremsstrahlung spectrum. The portal detector is a combination of a metal plate and a phosphor film. The function of the metal plate is to stop the energetic therapeutic X-rays and to produce secondary electrons; the escaped electrons will deposit energy in the phosphor film. We used a copper plate of various thicknesses (0–50 mm) and a phosphor film of Gd_2O_2S (0.1–5 mm) with reduced density of 3.67 g/cm^3 [2], [4], accounting for other compositions like polyurethane polymer-binder and air pockets. We used MCNP4B code again to simulate the interactions of X-rays and secondary electrons in the metal plate and phosphor film. The resulting AED of the phosphor film for various thicknesses of the metal plate and the phosphor film was used to estimate the energy moments and performance quantities discussed above by simple numerical integration and division.

To account for the spatial spread of scattered X-rays and secondary electrons in the phosphor film, leading to the DQE(f), the local distribution of energy absorption was estimated in predefined voxels of the phosphor layer in a simulation [7]. Then, the center point of each cell was assumed to be the representative position of the isotropic optical photon radiator, of which intensity is proportional to the absorbed energy of the whole cell [7]. Finally, the DQE(f) was calculated using the frequency-dependent quantum accounting theory [12], [13].

To confirm our simulation results, we conducted several experimental measurements such as the relative sensitivity and spatial resolution of the handmade detector with the X-ray beam from a 6-MV LINAC. The detailed experimental procedures can be found in [14]. In addition, some data from Munro's calculation and measurements [4], [5], [13] were used for the comparison with our results.

[1] Siemens Digital Mevatron KD, Serial # M2498.

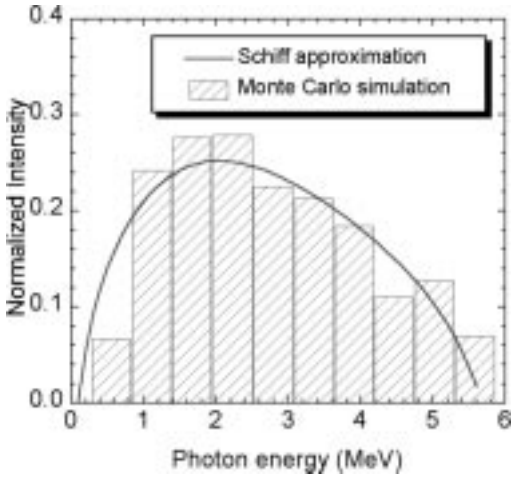

Fig. 1. Normalized Bremsstrahlung spectrum from the gold target of a 6-MV LINAC with the incident electron kinetic energy of 5.58 MeV. The intensity spectrum calculated by Schiff formula is also included.

III. Results and Discussion

A. Bremsstrahlung X-Rays

A simulated intensity spectrum of Bremsstrahlung X-ray beam produced from a 6-MV LINAC is presented in Fig. 1. All components of LINAC-head are considered in this simulation, such as the gold target including the cooling system, the primary collimator, a flattening filter, and a dose chamber. To confirm the simulation reliability, the Schiff intensity spectrum [15], which is widely used in the analysis of experimental results in high-energy or accelerator physics, was also calculated and included in the same figure. The mean energy of X-rays is 1.57 MeV. In the first energy bin or below 558 keV, the simulation underestimates the intensity. This discrepancy can be understood as the effect of the electron energy cutoff at 500 keV used in the simulation. However, since the Bremsstrahlung radiation yield at the energy below 500 keV is less than 5.3% in gold, the application of this energy cutoff is tolerable.

B. X-Ray Absorption

For incident Bremsstrahlung X-rays, Figs. 2 and 3 show the quantum and energy absorption efficiency, respectively, as a function of the metal thickness for three cases of phosphor thicknesses. These were calculated using the energy spectrum of Bremsstrahlung X-rays rather than the intensity spectrum shown in Fig. 1. These X-ray absorption efficiencies are very sensitive to the phosphor thickness, as expected. As shown in the figures, the energy absorption, resulting in the final signal output of phosphor, is largely enhanced by the introduction of metal plate even for a thickness of a few millimeters, while the quantum absorption is degraded. In addition, as the phosphor is thinner, the absorption efficiencies become independent of the metal plate

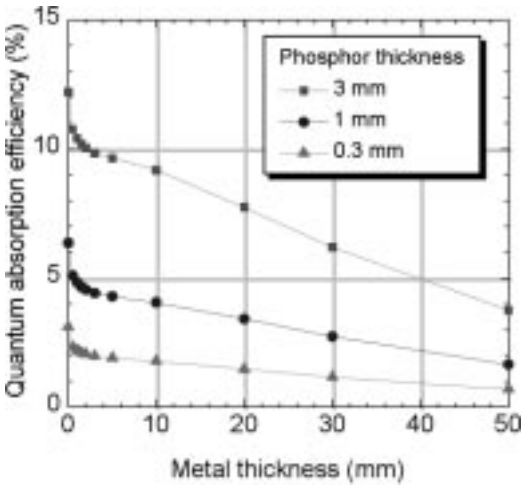

Fig. 2. Quantum absorption efficiencies of portal detectors. The use of a metal plate degrades the quantum absorption because the secondary quanta emitted from the metal plate gradually decrease.

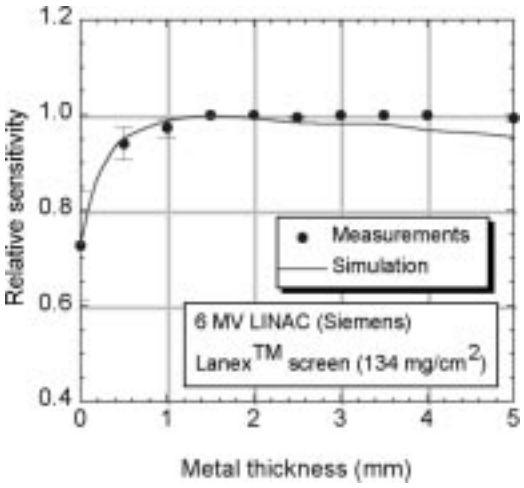

Fig. 4. Relative detector sensitivity as a function of the metal thickness. It is assumed that the signal output from the detector is directly proportional to the total energy deposited within the detector.

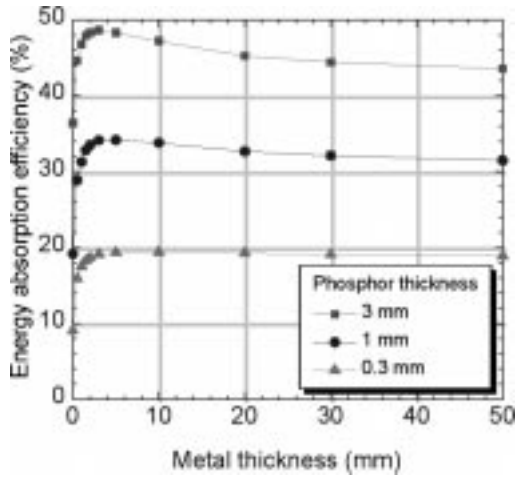

Fig. 3. Energy absorption efficiencies of the portal detector. The energy absorption is directly related to the detector signal output. The introduction of a metal plate largely enhances the energy absorption efficiency, which is strongly related to the secondary quanta fluence and their ranges within the detector.

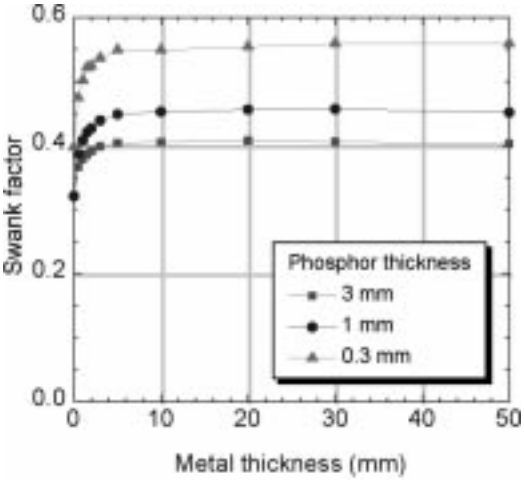

Fig. 5. Swank factors of the portal detector. Since the Swank factor is proportional to A_E^2, the overall feature is similar to the results of A_E. However, the dependency of the phosphor thickness is reversed because the variance of $S(E)$ becomes large as the phosphor thickness increases.

thickness because of the relatively long electron range in phosphor. However, the electron energy spectrum does not vary with the metal thickness because of the relatively short electron range in metal.

Since the light signal from the portal detector is directly proportional to the total absorbed energy within the detector, it can be estimated by multiplying the quantum and energy absorption. Therefore, we can easily expect from Figs. 2 and 3 that there exists a maximum value of the metal thickness. We irradiated the Lanex fast back screen (Eastman Kodak, Gd_2O_2S:Tb, 134 mg/cm^2) coupled to the copper plate with various thicknesses for the LINAC (Siemens) operated at 6 MV [14] and then compared with our simulation results. As shown in Fig. 4, the simulation result is in good agreement with the measured data.

C. Swank Factor

Generally, Swank factor is understood as the normalized DQE over the quantum efficiency. The calculated Swank factor, as presented in Fig. 5, has a saturation feature as a function of metal thickness that is similar to the energy absorption. But its magnitude decreases with the phosphor thickness, which is opposite to the energy absorption. These characteristics can be understood easily if we rearrange (4) as follows using the definition of A_Q and A_E:

$$A_S = \frac{A_Q (A_E)^2}{M_2}. \tag{7}$$

From the above expression, the Swank factor is a stronger function of the energy absorption than the quantum absorption, so its shape as a function of metal thickness follows the energy absorption. However, the variance of AED, M_2, becomes large when the phosphor thickness increases, so its magnitude has the reversed tendency as a function of phosphor thickness in comparison with the energy absorption.

D. Detective Quantum Efficiency

As mentioned before, the DQE is determined in terms of the quantum absorption and the Swank factor. As shown in Fig. 6,

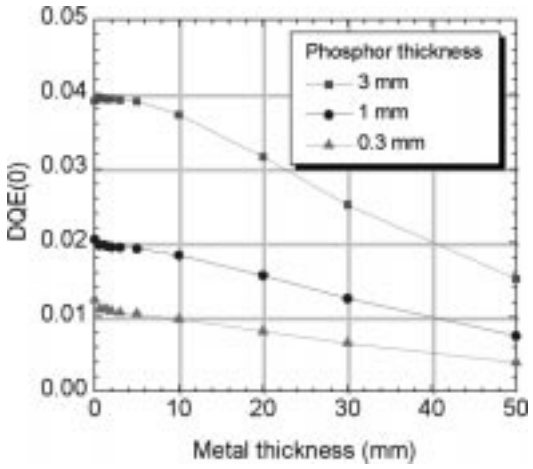

Fig. 6. Detective quantum efficiencies of the portal detector at zero spatial frequency. DQE results from the competition between A_Q and A_S. Above a 5-mm-thick metal plate, the quantum absorption dominates the DQE.

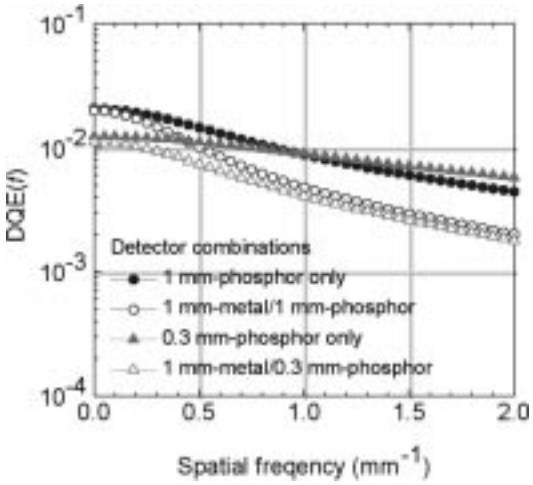

Fig. 7. DQE(f) for several portal detectors. It is noted that the presence of metal plate degrades the DQE(f).

the DQE follows the quantum absorption above the metal thickness of about 5 mm because the Swank factor is almost constant at that region. As concerns metal thickness (0–5 mm), the DQE is almost constant because of the rapid changing of the quantum absorption and the Swank factor. Thus, referring to the results of energy absorption for maximized signal output, the metal thickness of 5 mm is concluded to be an upper limit.

It is important to note that maximizing the DQE at zero spatial frequency is not sufficient in portal imaging. To be able to detect anatomical structures in the portal images reliably, it was reported that the DQE(f) should be maximized up to spatial frequencies of 0.4 mm^{-1} [16]. Considering the spatially absorbed energy distribution within the detector, the DQE(f), as shown in Fig. 7, was calculated for several portal detectors. The spatial distribution of the energy absorption in the portal detector was confirmed by the measurement of the line-spread function with a 6-MV X-ray beam [14]. From the simulation results, two important conclusions have been extracted: 1) the DQE values for a thinner phosphor layer are independent of spatial frequency and 2) the presence of a metal plate degrades the DQE for nonzero spatial frequencies. This conclusion is different from that of

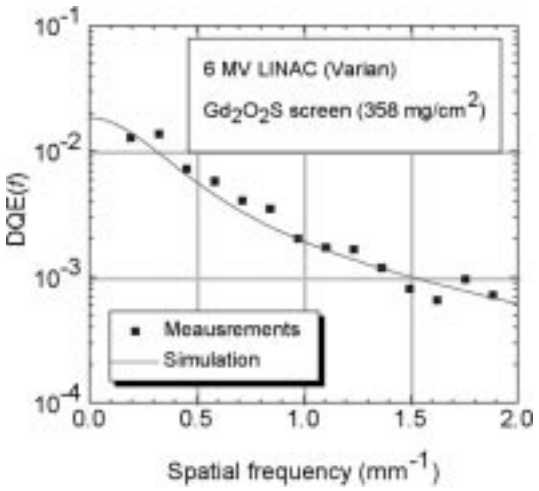

Fig. 8. DQE(f) for 1-mm Gd_2O_2S with 1-mm copper for a 6-MV X-ray beam from Varian LINAC. The simulated result is in excellent agreement with the experiment [5], [13]. The value of 0.018 at zero frequency is comparable to 0.017 by EGS4 code [4].

other literature based on monoenergetic X-ray approximations [4], [6].

To confirm our Monte Carlo calculation of DQE(f), we compared our results with theoretical and experimental data from the literature [5], [13]. For the comparison, we calculated the DQE(f) of their detector [4], [5], [13] for therapeutic X-ray beams from another type of 6-MV LINAC (Varian) [17]. Fig. 8 shows our calculation result, which has excellent agreement with the reference data. Munro's group [4] calculated DQE(0) by using EGS4 code, with a result of 0.017, which is very close to our value of 0.018 of DQE(f) at zero frequency.

IV. Conclusion

Using the Monte Carlo technique, we have studied X-ray absorption and its associated noise properties for a typical portal detector considering the realistic X-ray spectrum from a clinical LINAC. From the simulation results, we found the following.

1) There is an optimum thickness of the metal plate to maximize the detector sensitivity. For example, a 1.5-mm-thick copper plate for Gd_2O_2S screen with 134 mg/cm^2 (or 0.3 mm thick) gives the highest detection sensitivity for an X-ray beam from a 6-MV LINAC.
2) The DQE(f) becomes constant as the thickness of the phosphor layer decreases, which is due to the uniform energy deposition of secondary quanta of relatively long range, resulting in minimized absorption noise.
3) The use of a metal plate degrades the DQE(f) because the detector absorption noise is dominated by the quantum absorption.

The suggested simulation will be useful for the optimal design of typical portal detectors for different energy input. It also can be extended to any scintillating phosphor detector for other X-ray imaging systems such as flat-panel-type devices.

References

[1] P. Munro, "Portal imaging technology: Past, present, and future," *Sem. Radiat. Oncol.*, vol. 5, pp. 115–133, 1995.

[2] T. Radcliffe, G. Barnea, B. Wowk, R. Rajapakshe, and S. Shalev, "Monte Carlo optimization of metal/phosphor screens at megavoltage energies," *Med. Phys.*, vol. 20, pp. 1161–1169, 1993.
[3] B. Wowk, T. Radcliffe, K. W. Leszczynski, S. Shalev, and R. Rajapakshe, "Optimization of metal/phosphor screens for on-line portal imaging," *Med. Phys.*, vol. 21, pp. 227–235, 1994.
[4] D. A. Jaffray, J. J. Battista, A. Fenster, and P. Munro, "Monte Carlo studies of x-ray energy absorption and quantum noise in megavoltage transmission radiography," *Med. Phys.*, vol. 22, pp. 1077–1088, 1995.
[5] J. Bissonnette, I. A. Cunningham, and P. Munro, "Optimal phosphor thickness for portal imaging," *Med. Phys.*, vol. 24, pp. 803–814, 1997.
[6] C. Kausch, B. Schreiber, F. Kreuder, R. Schmidt, and O. Dossel, "Monte Carlo simulations of the imaging performance of metal plate/phosphor screens used in radiotherapy," *Med. Phys.*, vol. 26, pp. 2113–2124, 1999.
[7] H. K. Kim, G. Cho, Y. H. Chung, H. K. Lee, and S. C. Yoon, "Monte Carlo studies of metal/phosphor screen in therapeutic x-ray imaging," *Nucl. Instrum. Meth.*, vol. A422, pp. 713–717, 1999.
[8] R. K. Swank, "Absorption and noise in x-ray phosphors," *J. Appl. Phys.*, vol. 44, pp. 4199–4203, 1973.
[9] G. Cho, H. K. Kim, H. Woo, G. Oh, and D. K. Ha, "Electronic dose conversion technique using a NaI(Tl) detector for assessment of exposure dose rate from environmental radiation," *IEEE Trans. Nucl. Sci.*, vol. 45, pp. 981–984, 1998.
[10] J. F. Briesmeister, "MCNP-A general Monte Carlo N-particle transport code, version 4B," LANL, LA-12 625-M, 1997.
[11] B. L. Helmer, private communication, Siemens Medical Systems, Inc., Apr. 1998.
[12] I. A. Cunningham, M. S. Westmore, and A. Fenster, "A spatial-frequency dependent quantum accounting diagram and detective quantum efficiency model of signal and noise propagation in cascaded imaging systems," *Med. Phys.*, vol. 21, pp. 417–427, 1994.
[13] J. Bissonnette, I. A. Cunningham, D. A. Jaffray, A. Fenster, and P. Munro, "A quantum accounting and detective quantum efficiency analysis for video-based portal imaging," *Med. Phys.*, vol. 24, pp. 815–826, 1997.
[14] Y. H. Chung, H. K. Kim, G. Cho, S. K. Ahn, H. K. Lee, and S. C. Yoon, "Characterization of x-ray detector for CCD-based electronic portal imaging device," *J. Biomed. Eng. Res.*, vol. 21, pp. 119–127, 2000.
[15] G. E. Desobry and A. L. Boyer, "Bremsstrahlung review: An analysis of the Schiff spectrum," *Med. Phys.*, vol. 18, pp. 497–505, 1991.
[16] F. Kreuder, B. Schreiber, C. Kausch, and O. Dossel, "A structure based method for on-line matching of portal images for an optimal patient set-up in radiotheraphy," *Phillips J. Res.*, vol. 51, pp. 317–337, 1998.
[17] S. S. Kubsad, R. Mackie, M. A. Gehring, D. J. Misisco, B. R. Paliwal, M. P. Mehta, and T. J. Kinsella, "Monte Carlo and convolution dosimetry for stereotactic radiosurgery," *Int. J. Rad. Oncol. Biol. Phys.*, vol. 19, pp. 1027–1035, 1990.